NUMERICAL PREDICTION OF ATMOSPHERIC MIXED LAYER VARIATIONS OVER THE GULF COAST REGION DURING NOAA/ARL JSU METEOROLOGICAL FIELD EXPERIMENT SUMMER 2009 - SENSITIVITY TO VERTICAL RESOLUTION AND PARAMETERIZATION OF SURFACE AND BOUNDARY LAYER PROCESSES

William R. Pendergrass, LaToya Myles, Christoph A. Vogel
(NOAA/Air Resources Laboratory/Atmospheric Turbulence & Diffusion Division, Oak Ridge, TN)
and
Venkata Bhaskar Rao Dodla* , Anjaneyulu Yerramilli, Hari Prasad Dasari , C.V. Srinivas, Julius M Baham, Robert Hughes, Chuck Patrick, John Young, and Shelton Swanier
(Trent Lott Geospatial Visualization Research Centre, Jackson State University, Jackson MS 39204, USA)

ABSTRACT

Prediction of the mixed layer characteristics is important for generating the atmospheric dispersion characteristics using air quality models. The height of the mixed layer indicates the depth of the atmosphere over which the emissions could be diluted. It is known that the mixed layer height has diurnal variation and is influenced by local topographical and land use features. The present study aims to understand the utilization of the different parameterization schemes of the planetary boundary layer (PBL) and surface processes in the prediction of the characteristics of the PBL. For this purpose a high resolution mesoscale atmospheric model was used to predict the three dimensional atmospheric features over the Gulf coast region during 16-19 June 2009, when special observations were collected as a part of NOAA/ARL JSU/TLGVRC meteorological field experiment.

ARW (Advanced Research WRF) model was designed to have nested two-way interactive three domains with 36, 12 and 4 km resolutions, with the inner most domain covering the entire Gulf Coast region. The initial and boundary conditions were provided from NCEP FNL data available at 1 degree interval and the boundary conditions were updated at every 6 hours. The model was integrated for 48 hours starting from 00 UTC of each day starting from 15 June up to 00 UTC of 18 June 2009. Six sensitivity experiments were performed with the choice of thermal diffusion, NOAH-LSM and RUC schemes for surface processes and YSU and MRF schemes for PBL. Separately, three experiments were performed with three different vertical resolutions (i.e.) 27, 42 and 63 vertical levels.

As a part of joint NOAA-ARL and JSU-TLGVRC Meteorological Field Experiment Summer 2009, special radiosonde observations were collected at 5 times of 1400, 1600, 1800, 2000 and 2200 UTC for four consecutive days from 16 to 19 June, 2009 at the two locations, normal to the Mississippi Gulf Coast, of Harrison County School (30.5N,89.1W) and Wiggins Airport (30.8N,89.13W). The main objective of this field experiment was to understand the characteristics of the planetary boundary layer (PBL) over the Gulf Coast region.

The model output from the different experiments was analyzed and the thermodynamic fields corresponding to the locations of Harrison County High School and Wiggins Airport were retrieved. The vertical distributions of temperature and humidity fields along with wind variations were compared with the observations collected at these two locations during the field experiment. Specifically the characteristics of the mixed layer as obtained from the different sensitivity experiments were compared with the observations to assess the relative importance of the combination of surface and PBL schemes. The model results indicate distinct variations between different predictions. The results indicate that the PBL processes play a significant role as compared to the surface processes. Of all the sensitivity experiments, the combination of YSU scheme for PBL and RUC scheme for surface processes produce the best prediction. In general, the decrease of the temperature with height capped by a small inversion layer and then gradual decrease of temperature in the free atmosphere could be well simulated. Sensitivity experiments with respect to vertical resolution show improvement in the prediction of vertical thermodynamic structure with increased vertical resolution below 800hPa level.

1. INTRODUCTION

The troposphere, lowest part of the atmosphere, can be divided into two parts: a planetary boundary layer (PBL), extending upward from the surface to a height that ranges anywhere from 100 to 3000 m, and above it, the free atmosphere. The thickness (depth) of the PBL is not constant. The PBL is the major supplier of heat and moisture and temperature and moisture advections are important in weather forecasting. An increase of moisture and heat to the PBL will cause the atmosphere to become more unstable. The top of the PBL is often marked with a temperature inversion, a change in air mass, and change in wind speed and/or a change in wind direction. Inversions traps air within the PBL and do not allow convection to occur into the middle and upper atmosphere. During the day, the PBL often mixes out to the dry adiabatic lapse rate, especially on clear days. At nights with clear skies the opposite occurs as the surface radiationally cools, creating a large temperature inversion throughout the entire PBL.

Various types of models have been used to examine the PBL processes and their parameterization, since these circulations are typically smaller than the grid mesh used in weather prediction models. Atmospheric and oceanic PBLs serve as the interface between all of the system components, atmosphere, ocean, land, and biosphere and proper PBL parameterization schemes are needed to

*Corresponding author E-Mail:
venkata.b.dodla@jsums.edu

accurately link all of these components. These were dependent primarily on mixed-layer (bulk) modeling and second-order turbulence closure PBL modeling. Field experiments were designed to elucidate the effects of terrain and inhomogeneities in surface characteristics. *Lenschow* (1994) provided a good review on advances in measurement techniques, without covering remote sensing development. Interest in studying complex PBL processes that occur over non-homogeneous surfaces is increasing as the understanding of these complicated regimes and development of parameterization schemes is limited. Another constraint is that the PBL often undergoes rapid temporal or spatial changes, which makes it difficult to average by smoothing or parameterization over time or space. These emphasize the need for a denser data set (which is too expensive) before PBL processes could accurately be represented in models. A number of studies in which atmospheric models were integrated with air quality models for the estimation of pollutant concentration and dispersion show the role of PBL in air quality modeling (*Anjaneyulu*, 2008, 2009; *Challa* 2008, 2009).

Meteorological quantities that directly influence the air quality simulations include wind field, temperature profiles, water vapor mixing ratio, boundary layer depth, turbulent fluxes, surface pressure, shortwave radiation, rainfall/ precipitation in the lowest 2 or 3 km (*Hanna, 1994; Seaman, 2000; Mao et al., 2006*) of the troposphere. Several parameters in a meteorological model influence its performance, which include the model initial conditions, physical process parameterizations and spatial and temporal resolutions (*McQueen et al., 1995; Pielke and Uliasz, 1998; Warner et al., 2002; Berg et al., 2005; Jimenez et al., 2006*). Of the various atmospheric physical processes, the land surface and planetary boundary layer processes are interactive and play important roles in the simulation of the lower atmospheric turbulence, winds and other state variables. The land surface model (LSM) calculates the heat and moisture fluxes over land, sea-ice points and provide a lower boundary condition for the vertical transport in the PBL. The development and growth of the PBL depends on the surface heat and moisture fluxes, their upward mixing by the turbulent eddies. All of these phenomena influence the atmospheric transport and diffusion processes and hence are important in air quality modeling. Thus it is important to evaluate model performance for identification of a physically reasonable combination of land surface and PBL schemes for air quality simulations. Extensive field observations are needed to study the behavior of the PBL and the Joint NOAA/ARL- JSU/TLGVRC Summer-2009 Field Experiment was taken up with a view to study the PBL characteristics over the Mississippi Gulf Coast region during summer season.

The present study is an attempt to study the sensitivity of the PBL and land surface processes in the simulation of the characteristics of PBL over the Mississippi Gulf Coast region during the period of Summer-2009 field experiment. A description of the field experiment is provided in Section2, followed by the details of numerical model design and experimentation in Section 3 and the results in Section 4.

2. FIELD EXPERIMENT

A joint special observation field experiment was conducted by NOAA/ARL and JSU/TLGVRC for a 5-day period during 16-20 June 2009 near Gulf Port of the Mississippi State. This observation program is taken as a part of the ongoing NOAA sponsored ADP program at JSU/TLGVRC since 2006 and that Mississippi Gulf Coast houses many industries that release pollutants. The ADP program has the main objective of studying the atmospheric dispersion of the important pollutants that are being released and spread in this region affecting the habitants. Radiosonde balloons were released at 5 times during daytime hours of 09, 11, 13, 15 and 17 hours of Central US time, which correspond to 14, 16, 18, 20 and 22 UTC, on all the five days during 16-20 June 2009 at two selected locations. These two locations are Harrison County School (30.5N, 89.1W) and Wiggins Airport (30.8N, 89.13W), which are 30 miles apart on the longitude of 89W and nearly perpendicular to the Gulf Coast (Figure 1). These observations were planned to probe and study the evolution of sea breeze and the planetary boundary layer characteristics over the Mississippi Gulf Coast region. The Radiosonde balloons were given ascent so as to reach 12-16 km in about an hour. The sensors attached to the balloon were sending the atmospheric data of temperature and humidity and balloon location through GPS (to yield wind direction and speed) at every 10 sec interval, which is at a vertical resolution of about few tens of meters. This raw data was directly loaded into a computer storage system and the vertical profiles of temperature and humidity were continuously updated every 30 sec through use of special meteorology application software (like RAOB). The observations were then subject to a quality control check at NOAA and were made available for analysis.

3. MODEL AND NUMERICAL EXPERIMENTS

The details of the mesoscale atmospheric model, and the details of the numerical experiments performed are presented in this section.

3a. *Description of Atmospheric Model*

ARW model is used to produce the atmospheric fields at a high resolution over the study region for the desired time period. WRF (Weather Research and Forecasting) mesoscale atmospheric modeling system has been developed and sourced from National Center for Atmospheric Research (NCAR), as the next generation model after MM5, incorporating the advances in atmospheric simulation system suitable for a broad range of applications. WRF is available with two different dynamic cores one as the Advanced Research WRF (ARW) and the other as the Non-hydrostatic Mesoscale Model (NMM). This model system has versatility to choose the domain region of interest; horizontal resolution; interactive nested domains and with various options to choose parameterization schemes for convection, planetary boundary layer (PBL), explicit moisture; radiation and soil processes. ARW is designed to be a flexible, state-of-the-art atmospheric simulation system that is portable and efficient on available parallel computing platforms and a detailed description was provided by *Skamarock et al. (2008)*. ARW is suitable for use in a broad range of applications across scales ranging from meters to thousands of kilometers. ARW model system was used in this study for its accurate numerics, higher order mass conservation characteristics and advanced physics. The model consists of fully compressible non-hydrostatic equations and the prognostic variables include the three-dimensional wind, perturbation quantities of pressure, potential temperature, geo-potential, surface pressure, turbulent kinetic energy and scalars (water vapour mixing ratio, cloud water etc). The model equations are formulated using mass-based terrain following coordinate system, and solved in Arakawa-C grid using Runge–Kutta third order time integration techniques. The model has several options for spatial discretization, diffusion, nesting and lateral boundary conditions. The ARW Solver is the key component of the modeling system, which is composed of several initialization programs for idealized, and real-data simulations, and the numerical integration program. ARW supports horizontal nesting that allows resolution to be focused over a region of interest by introducing an additional grid (or grids) into the simulation with the choice of one-way and two-way nesting procedures. The model system provides a choice of parameterization schemes for physical processes of microphysics, cumulus parameterization, planetary boundary layer (PBL), land surface model and radiation.

3b. Numerical Experiments

For the present study, ARW model was configured with three, two-way interactive nested domains, with outer domain at 36 km resolution, middle domain at 12 km resolution and inner domain at 4 km resolution and 42 vertical levels. The details of the design and adaptation of ARW model, for the present study, are given in Table 1 and the model domains are shown in Figure 2. ARW model was integrated for a 48-hour period starting from 00 UTC of each day of 15 to 19 June 2009. The initial and time varying boundary conditions required for the model integrations were taken from NCEP FNL data available at 1 degree interval and at 6-hour interval. The boundary conditions are updated at every 6 hour interval (i.e.) at 00, 06, 12 and 18 UTC during the period of model integration. The model topography and land use for the three model domains were taken from USGS data sources. Six numerical experiments were performed with the combinations of two PBL schemes and three schemes for surface processes and the model derived outputs were analyzed for the times at which observations were made during the field experiment.

4. RESULTS

As mentioned in the earlier section, sensitivity experiments were conducted with two schemes of planetary boundary layer (PBL) (YSU and MRF) and three schemes for surface processes (thermal diffusion, NOAH-LSM and RUC-LSM). The results from the six experiments were analyzed to obtain the model predicted vertical variations of temperature, relative humidity (RH) and wind corresponding to the times for which observations were available. The model results were interpolated for the two station locations of Harrison County School and Wiggins Airport. Through model results were available four days period (i.e.) 16-19 June, 2009 the results are presented and discussed only for 18 June, 2009. Similarly the results are shown only for the observation times of 14 and 20 (or 22) UTC as representative of the morning and evening local times of 09 and 15 (17) CDT.

4a. Harrison County School

The vertical profiles are shown below 600 hPa level for all the six experiments along with the observations. The profiles below 850 hPa level were shown separately for the experiments with each of the three surface schemes for better comparison and evaluation of the boundary layer structure.

The vertical variations of temperature below 850 hPa level are shown in Figure 3 and Figure 4. The results were presented for the experiments with each of the two PBL schemes in combination with each of the three schemes of surface processes. With all the three schemes of surface processes, experiments with MRF PBL scheme show better features than with YSU PBL scheme. At 14 UTC, the model simulated vertical profiles of temperature below 600 hPa level shows (Figure 3d) very good similarity with observations, except for sharp variations in shallow layers within and at the top of the boundary layer. The model simulated lapse rate significantly correlates with the observations. The simulation at 950 hPa level was better represented in Figures 3a-c. Below 850 hPa level, observations show a decrease of temperature up to 980 hPa, increase up to 940 hPa, decrease between 940 hPa and 900 hPa, increase between 900-890 hPa levels and decrease above. The experiments with MRF PBL scheme simulates decrease of temperature below 980 hPa and above 940 hPa with a near isothermal layer between 980 and 940 hPa levels. Contrastingly experiments with YSU PBL scheme show similar features but with a shallow isothermal layer between 975- 960 hPa levels.

It is clearly noted that the model profiles from the three different schemes of surface processes are nearly identical indicating that the simulations are not sensitive to the surface processes and that PBL processes are important. At 20 UTC, observations show sharp decrease below 850 hPa level and above 800 hPa levels with an inversion layer in between a thin shallow inversion layer is noted at 650 hPa level. The model could not simulate these two inversions properly. The model simulated low level inversion to be at 950 hPa level as compared to 850 hPa level in the observations. The model simulations of temperature profiles, below 850 hPa level, show decrease of temperature but with smaller lapse rate compared to the observations. A comparison of the experiments with the two PBL schemes indicate better simulation with MRF PBL scheme as the inversion layer is predicted at a higher level than with YSU PBL. However, both the schemes predict the inversion layer much lower than the observations at this time.

At 14 UTC, observations show an increase of RH below 950 hPa level, a decrease up to 700 hPa and increase above. Correspondingly the model simulates an increase below 950 hPa level and a gradual decrease up to 750 hPa level and gradual increase above. Finer features above 850 hPa are shown in Figure 3(a,b,c). At this time, vertical profile of RH below 850 hPa level shows a gradual increase from 950 hPa, rapid decrease in a shallow layer both 950-940 hPa levels, nearly constant RH between 940-900 hPa levels, sudden rapid decrease in a thin shallow layer near 900 hPa level and near constant RH above. All the experiments with MRF PBL scheme show gradual decrease below 970 hPa level and nearly constant RH above 940 hPa level with gradual decrease between 970-940 hPa levels. Contrastingly all the experiments with YSU PBL scheme show increase of RH from surface up to 975 hPa, steep decrease up to 950 hPa level and gradual decrease above 950 hPa level. Thus the MRF PBL scheme provides better simulation with thicker layer of decreasing RH and a constant RH layer above 940 hPa level. Nearly identical vertical distribution of RH for all the three surface schemes with respect to both the MRF and YSU PBL schemes indicate that the simulation is not sensitive to the surface processes and that PBL schemes play an important role.

At 20 UTC, the observations show increase of RH up to 850 hPa level, sharp decrease within a shallow layer between 850-825 hPa levels and gradual increase above. The model simulation shows increase up to 950 hPa level, sharp decrease within a shallow layer near 950 hPa level, gradual decrease up to 850 hPa, near constant RH between 850-700 hPa levels and gradual increase above. This shows that the model simulates inversion layer much below at 925 hPa level as compared to 850 hPa in the observations. Better simulation with MRF PBL is shown in Figure 3a-c. Experiments with MRF PBL simulate the inversion layer to be higher than with YSU PBL scheme. This is same with all the surface schemes and the differences in the height of the PBL are attributed to the differences in the PBL schemes.

The vertical variation of wind speed at 14 UTC, shows large variations with shallow layers below 600 hPa level. The model simulations show similar values of the wind speed but with smaller magnitudes below 800 hPa level and with agreeing magnitudes above 800 hPa level as compared to observations. All the experiments simulate similar features but with differences in magnitude below 850 hPa level. Figure (a,b,c) show the simulation of finer features of the vertical variations below 850 hPa level. Experiments 2, 3 and 6 simulate higher magnitudes of 3 m/s as compared to a maximum of 2 m/s with the experiments of 1, 4 and 5. This indicates that MRF PBL simulates higher wind speed with magnitude more near to the observations as compared to the experiments with YSU PBL scheme. At 20UTC, the observed wind speed ranges between 0-4 m/s and the model simulates the vertical variations with magnitudes similar to the observations. The variations below 850 hPa level show that the model could not simulate the sharp variations between 975-925 hPa levels. However experiments with MRF PBL have lesser errors in magnitudes as compared to the experiments with YSU PBL schemes. These results show the ability of the model to predict the gross features of the vertical variations and its inability to predict finer details.

The vertical variation of wind direction at 14UTC shows that the model simulates the variations in the wind direction as similar to the observations. Below 600 hPa level all the experiments predict backing of wind with height as of the observations. The finer structure below 850 hPa level (Figure a, b and c) shows that the experiments with MRF PBL scheme simulates the finer features better than the YSU PBL scheme. Below 600 hPa level, the model simulates all the gross features agreeing with the observations with the wind direction to be nearly north below 850 hPa level and backing of wind above 850 hPa level. However, experiments with MRF PBL show better simulation below 850 hPa level as compared to the YSU PBL scheme. All the experiments predict wind directions in the northwest quadrant (270-360 degrees) with MRF PBL scheme simulating wind directions more near to the observations.

4b. Wiggins Airport

For the location at Wiggins Airport, similar analyses as of the Harrison County School, were performed and the results are presented briefly as follows. Most of the features are the same as of the Harrison County School and so only few plots are presented.

At 14 UTC, the observations of the vertical profile shows gradual decrease of temperature with two embedded inversions in the shallow layers between 975-920 hPa and 900-875 hPa levels. The model simulations show an inversion between 980-950 hPa levels with general decrease of temperature from surface to 600 hPa level. The model simulated lapse rate agrees with that of the observations. Figure depicting the finer structure below 850 hPa level, shows that experiments 2,3 and 6 simulates the inversion to be between 950-925 hPa with MRF PBL whereas all the experiments with YSU PBL scheme simulate the inversion between 975-950 hPa levels.

At 22 UTC, observations show inversion in a thin shallow layer between 850-800 hPa levels, whereas the model simulations show the inversion around 950 hPa level. This indicates the model’s inability to predict the increase of PBL height associated with increasing daytime heating. MRF PBL scheme simulates the inversion at a higher level than the YSU PBL scheme.

The observations of the vertical variation of RH at 14 UTC of 20090618, indicate near constant RH up to 900 hPa, sudden decrease in a thin shallow layer at 900 hPa level, near constant RH between 900-700 hPa level and a gradual increase above. The model experiments show similar variations as of the observations with certain limitations. The model simulates increase of RH from the surface up to 980 hPa as compared to an increase up to 975 hPa in the observations; decrease from 980 hPa to 960 hPa as compared to the sudden decrease at 920 hPa in the observations. The model simulations reasonably agree with the observed RH variations above 900 hPa level. Significantly, the model simulates increasing of RH above 700 hPa level coinciding with the observations. A detailed analysis of the vertical variation of RH below 850 hPa show that all the 3 experiments with MRF PBL scheme simulate the vertical variations better than those with YSU PBL scheme, as the MRF PBL scheme predicts higher PBL height than with YSU PBL scheme and closer to the observations. At 22UTC, observations show increase of RH up to about 850 hPa level and a sudden decrease of RH in a thin shallow layer at 850 hPa level indicating the increase of height of PBL at this time as compared to 14 UTC. All the model simulations predict increase up to 950 hPa and a decrease between 950-850 hPa level. This indicates the simulations of the inversion layer to be larger than the observations. However, the simulations of the increase at lower levels and decrease up to 850 hPa level is to be taken as the model's capability within the limitation of the adapted vertical resolution. Analysis of the finer structure below 850 hPa level confirms this feature and also indicates the superior performance of the MRF PBL scheme which predicts the height of the PBL more nearer to the observations.

The vertical variations of wind speed below 600 hPa level, at 14 UTC, shows that the observations of wind speed have a magnitude varying between 4-6 m/s below 800 hPa level; wind speed decreasing to 0.5 m/s at 725 hPa level and gradual increase above. Correspondingly the model simulations show increase of wind speed up to 3 m/s at 925 hPa level; remain nearly constant (2-2.5 m/s) between 950-700 hPa level; and gradually increase above 700 hPa level. At 22 UTC, the magnitude of wind speed decreases to be around 2 m/s up to 700 hPa level and then increase to about 3 m/s above 700 hPa level. The model simulations show the wind speed to be 2-4 m/s below 980 hPa level, decrease to 0.5 m/s at 800 hPa level and gradually increase above. All the gross features of vertical variations of wind speed coincide with the observations.

At 14 UTC, observations of wind direction show values between 230-280 degrees below 750 hPa level and 100-150 degrees above 700 hPa level. Observations show sharp variations in the layer between 750-700 hPa level. Correspondingly the model simulates the wind direction to be 250-300 degrees below 850 hPa level and 100-150 degrees above 700 hPa level and with gradual decrease of wind direction between 850-700 hPa levels. At 22 UTC, observations have the wind direction between 250-350 degrees below 750 hPa level and around 250 degrees above 700 hPa level. The model simulations show the wind direction to be 300-360 degrees below 850 level and between 100-150 degrees above 750 hPa level. Thus the model could simulate the wind direction below 850 hPa level and above 700hPa level. However, the sharp variations between 850-700 hPa level could not be simulated by the model. At both 14 and 22 UTC, MRF PBL scheme simulates better than YSU PBL scheme with the wind speed and wind direction to more nearer to the observations.

5. CONCLUSIONS

Numerical model experiments were performed to study the sensitivity of model simulations to the parameterization schemes of PBL and surface processes using WRF ARW model. Altogether six experiments were conducted with two PBL schemes of MRF and YSU, and three surface process schemes of thermal diffusion, NOAH-LSM and RUC-LSM. The model simulations of the vertical variations of temperature, relative humidity and wind speed and direction below 600 hPa level, at the two locations of Harrison County School and Wiggins Airport, were compared with observations taken during the daytime periods of 16-19 June 2009. A preliminary study leads to the following conclusions.

1. The model could simulate the gross features of the vertical variations of the temperature, humidity and wind below 600 hPa level. However there are certain limitations which are attributable to the adapted vertical resolution.
2. The results indicate the PBL processes play dominant role in the evolution of boundary layer over the study region. Model simulations are not sensitive to the surface processes.
3. Of the two PBL schemes taken up for study, MRF PBL produced better simulation with respect to all the parameters of temperature, humidity and wind speed and direction.
4. The model could simulate the inversion layer at the top of PBL, as characterized by increase of temperature with height, and sharp decrease of RH. The model underestimates the increase of PBL height with increasing daytime.

The above analysis is preliminary and detailed investigation is in progress. This study emphasizes the need for conduct of special field observation experiments to understand the features of the coastal boundary layer characteristics. The field experiment produced valuable data and provided an opportunity to validate model simulations. This study points out some of the deficiencies of model simulation and the areas where improvements in parameterization of physical processes are needed. For eg. parameterization of surface physics is to be improved and higher vertical resolution is to be adopted.

6. ACKNOWLEDGMENT

This study is carried out as part of the ongoing Atmospheric Dispersion project (ADP) funded by National Oceanic and Atmospheric Administration (NOAA) through the U.S. Department of Commerce Grant #NA06OAR4600192.

7. REFERENCES

Anjaneyulu, Y., C. V. Srinivas, H. P. Dasari, L. D. White, J. M. Baham, J. H. Young, R. Hughes, C. Patrick, M. G. Hardy and S. J. Swanier. Simulation of Atmospheric Dispersion of Air-Borne Effluent Releases from Point Sources in Mississippi Gulf Coast with Different Meteorological Data. *Int. J. Environ. Res. Public Health*, **2009**, *6*, 1055-1074.

Anjaneyulu, Y., C. V.Srinivas, I. D., Jayakumar, J. Hariprasad, J. Baham, C. Patrick, J. Young, Hughes, L. D., White, M. G. Hardy and S. Swanier. Some observational and modeling studies of the coastal atmospheric boundary layer at Mississippi Gulf coast for

Air Pollution Dispersion assessment: *Int. J. Environ. Res. Public Health*, **2008**, *5(5)* 484-497.

Berg, L. K., and S.Zhong, Sensitivity of MM5-Simulated Boundary Layer Characteristics to Turbulence Parameterizations, *J. Appl. Meteor.*, **2005**,44 (9), 1467-1483

Challa, Venkatasrinivas, Jayakumar Indracanti, J. M Baham, R. Hughes, C. Patrick, J. Young, M. Rabbarison, S. Swanier, M. G. Hardy and Y. Anjaneyulu. Sensitivity of Atmospheric dispersion simulations by HYSPLIT to the meteorological predictions from a mesoscale model *Environ. Fluid Mechanics*, **2008**, 8:367-387.

Challa, Venkatasrinivas, Jayakumar Indracanti, J. M Baham, R. Hughes, C. Patrick, J. Young, M. Rabbarison, S. Swanier, M. G. Hardy and Y. Anjaneyulu. A Simulation Study of Meso-Scale Coastal Circulations in Mississippi Gulf coast for Atmospheric Dispersion. *Atmos. Res.,* ***2009**,* 91, 9-25.

Hanna, S.R. Mesoscale Meteorological Model Evaluation Techniques with Emphasis on Needs of Air Quality Models. in Meteorological Monographs: Mesoscale Modelling of the Atmosphere (eds. Roger A. Pielke and Robert P. Pearce) **1994**, Vol.25, No.47, American Meteorological Society, Boston, Massachusetts 02108.

Jimenez, P., O.Jorba, R.Parra, and J.M.Baldasano, Evaluation of MM5-EMICAT2000-CMAQ performance and sensitivity in complex terrain: High-resolution application to the northeastern Iberian Peninsula. *Atmos. Environ.* **2006**, 40, 5056-5072.

Lenschow DH. Micrometeorological techniques for measuring biosphere-atmosphere trace gas exchange. In: Mattoon PA, Harris RC, eds. *Biogenic trace gases: measuring emissions from soil and water.* Oxford: Blackwell Science, **1995**, 126-63.

Mao, Q., L.L.Gautney, T.M.Cook, M.E.Jacobs, S.N.Smith, and J.K. Kelsoe, Numerical experiments on MM5-CMAQ sensitivity to various PBL schemes, *Atmos. Environ*. **2006**, 40, 3092-3110.

McQueen, J.T., R.R.Draxler, and G.D.Rolph, Influence of grid size and terrain resolution on wind field predictions from an operational mesoscale model, *J. Appl. Meteor*. **1995**, 34 (10), 2166-2181.

Pielke, R.A., and M. Uliasz, Use of meteorological models as input to regional and musicale air quality models – limitations and strengths. *Atmos. Environ*. **1998**, 32, 1455-1466.

Seaman, N.L., and S.A. Micheleson, Mesoscale meteorological structure of a high-ozone episode during the 1995 NARSTO-Northeast study. *J. Appl. Meteor*. **2000**, 39, 1762-1784.

Skamarock, W.C., J.B. Klemp, J.Dudhia, D.O.Gill, D.M. Barker, M.G.Duda, X.-Y.Huang, W.Wang, and J.G.Powers, A Description of the Advanced Research WRF Version 3. NCAR Technical Note **2008**, NCAR/TN-475+STR. Mesoscale and Microscale Meteorology Division, National Center for Atmospheric Research, Boulder, Colorado, USA

Warner, T., R. Sheu, J.F.Bowers, R.I. Sykes, G.C. Dodd, D.S. Henn. Ensemble Simulations with Coupled Atmospheric Dynamic and Dispersion Models: Illustrating Uncertainties in Dosage Simulations. *J. Appl.Meteor*. **2002**, 41, 488-504.

Table 1: Details of WRF ARW model

Model Name	NCAR/NCEP WRF ARW VERSION 3		
Model type	Primitive equation, Non- hydrostatic		
Vertical resolution	41 sigma levels		
Two- way nested three domains			
Horizontal resolution	36 km	12 km	4 km
Domain of integration	93.0 W – 78.05 W 27.16 N – 34. 45 N	91.74 W – 81.92 W 28.5 N – 34. 45 N	90.28 W – 84.77 W 29.38 N – 32.54 N
Number of grids (W-E x S-N)	54 x 40	109 x 76	187 x 118
Radiation	Dudhia scheme for short wave radiation. Rapid Radiative Transfer Model for long wave radiation		
Surface physics	RUC Land- Surface Model		
Sea Surface Temperature	Real Sea Surface Temperatures		
Convection	Kain- Fritsch (KF-Eta).		
PBL	YSU		
Explicit moisture	WSM3 Simple Ice		

Figure 1. Location of the observation stations along the Mississippi Gulf Coast

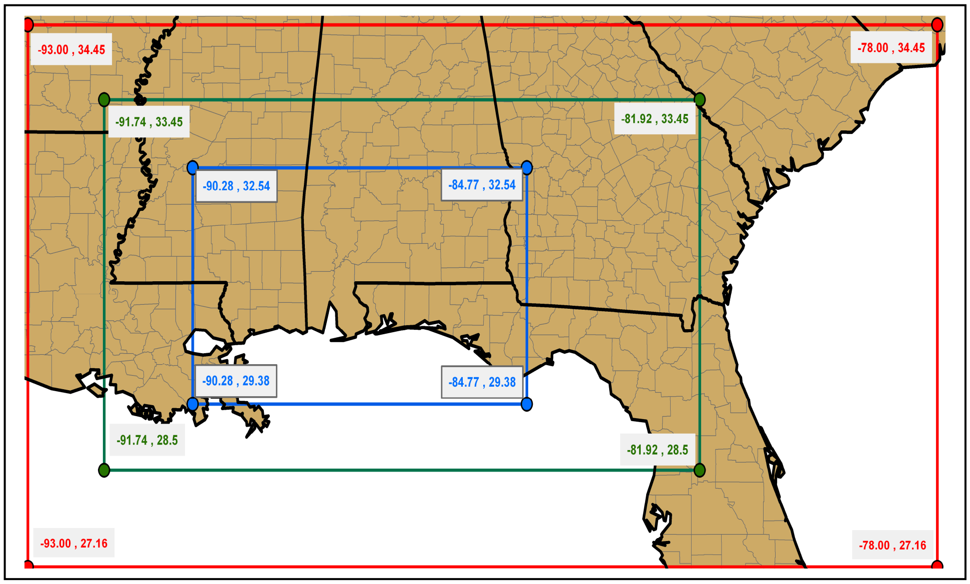

Figure 2. Model domains

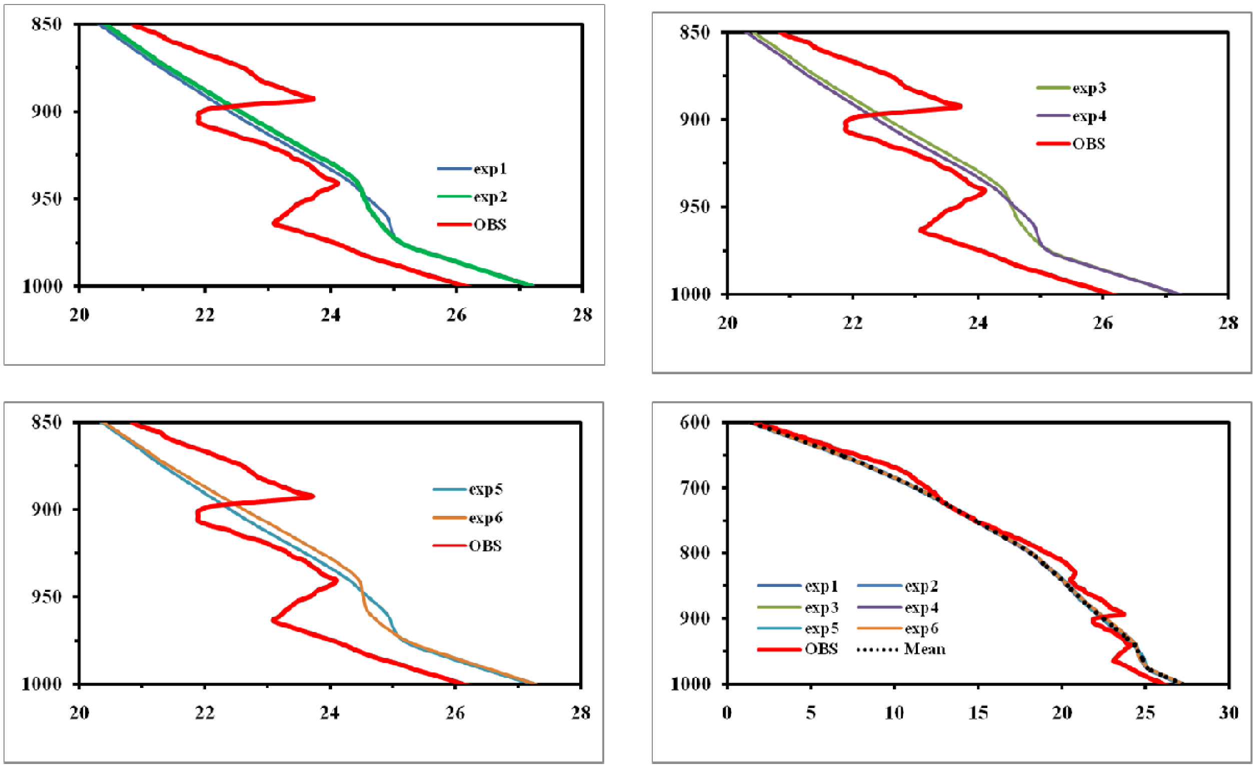

Figure 3. Model predicted vertical variation of temperature for the different sensitivity experiments along with the observations at the location of Harrison County School corresponding to 14 UTC of 18 June 2009

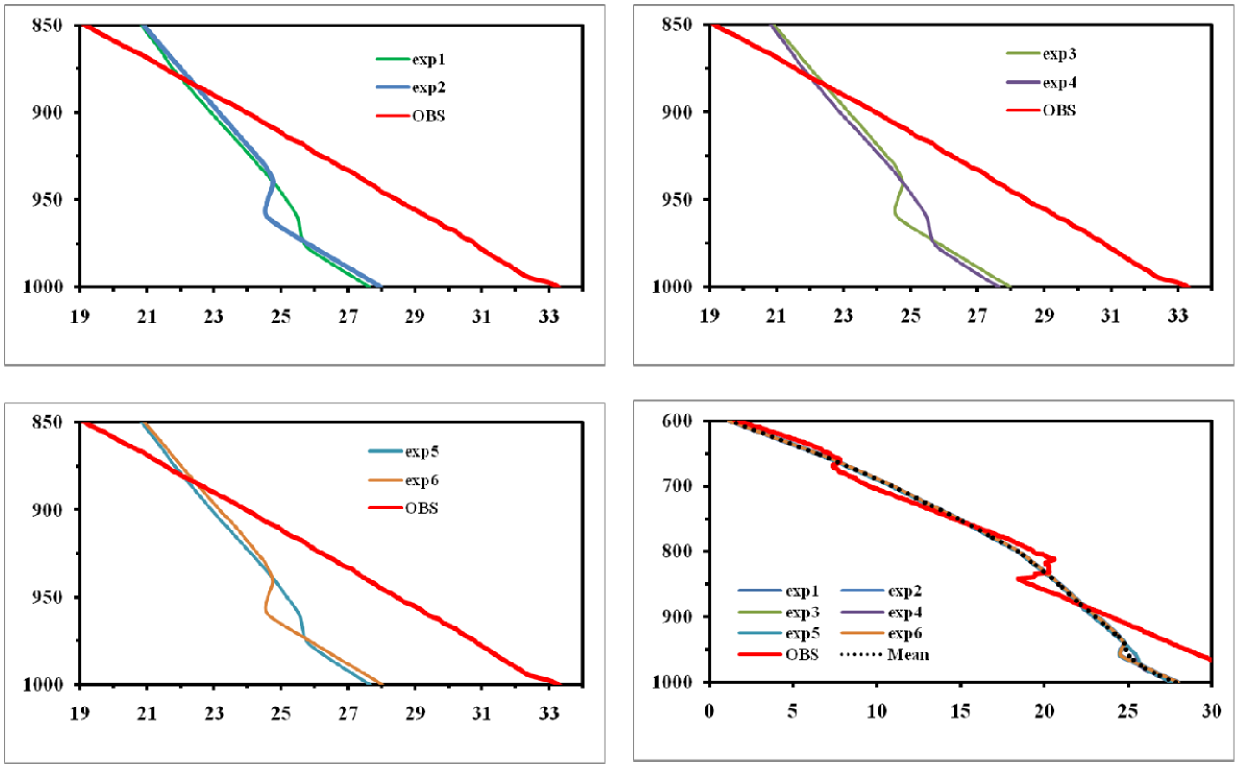

Figure 4. Model predicted vertical variation of temperature for the different sensitivity experiments along with the observations at the location of Harrison County School corresponding to 20 UTC of 18 June 2009

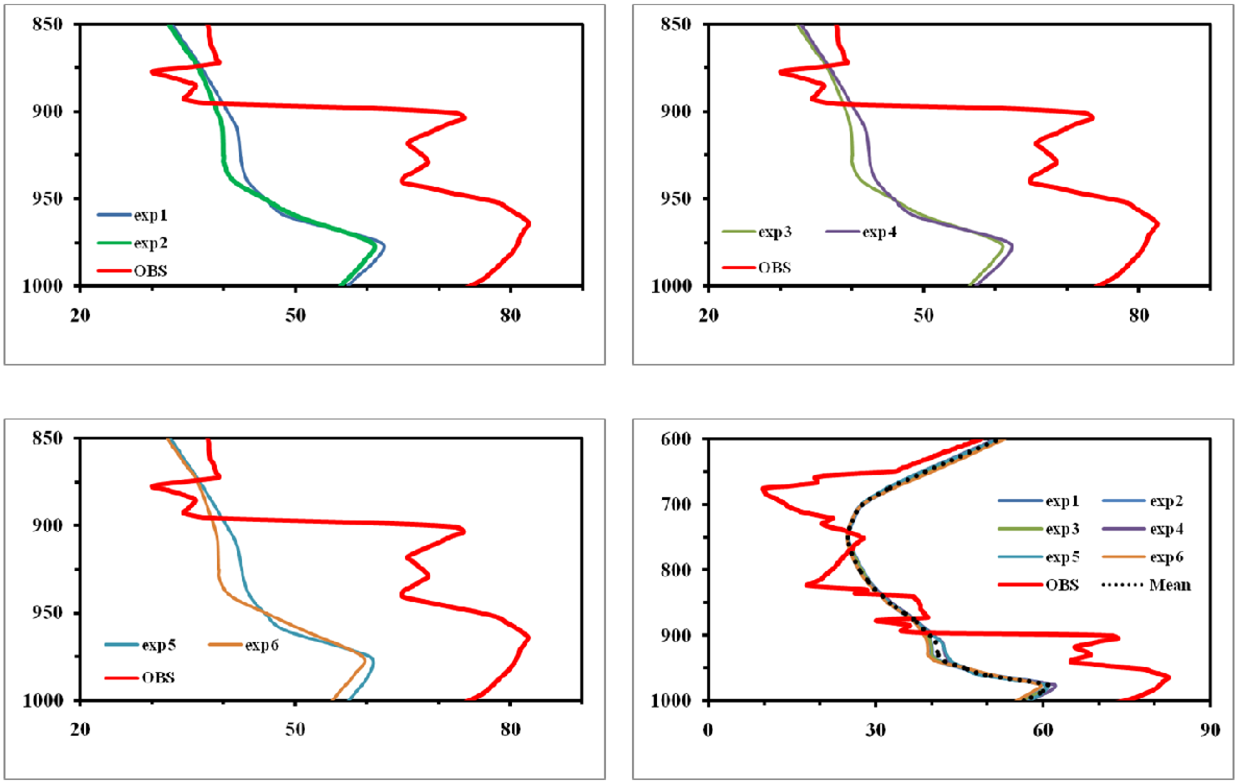

Figure 5. Model predicted vertical variation of relative humidity (%) for the different sensitivity experiments along with the observations at the location of Harrison County School corresponding to 14 UTC of 18 June 2009

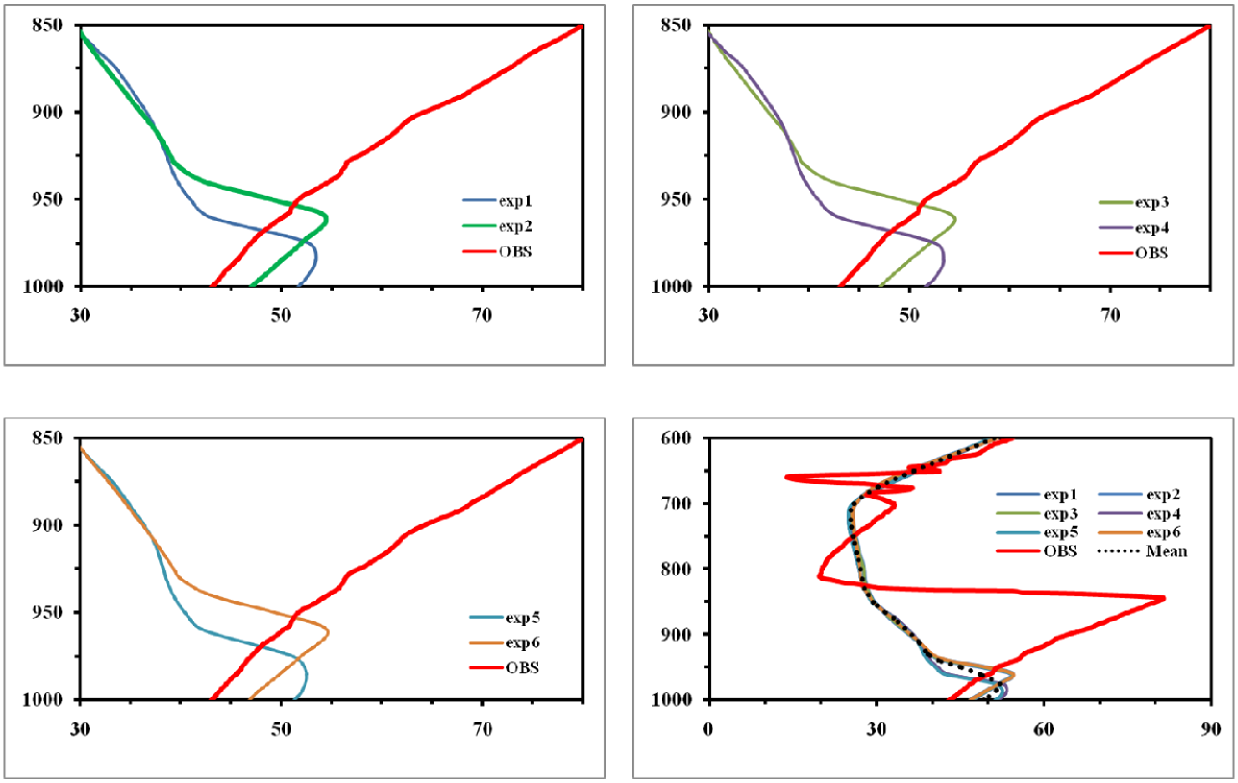

Figure 6. Model predicted vertical variation of relative humidity (%) for the different sensitivity experiments along with the observations at the location of Harrison County School corresponding to 20 UTC of 18 June 2009

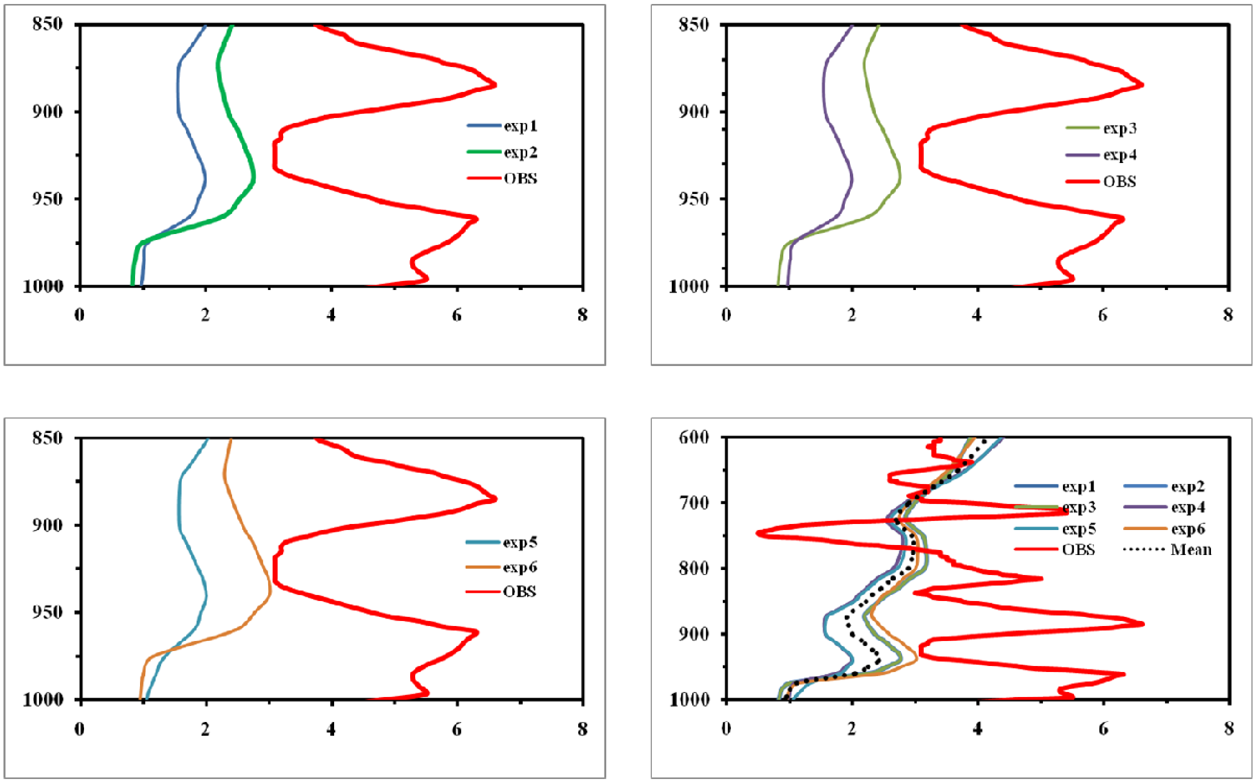

Figure 7. Model predicted vertical variation of wind speed (m/s) for the different sensitivity experiments along with the observations at the location of Harrison County School corresponding to 14 UTC of 18 June 2009

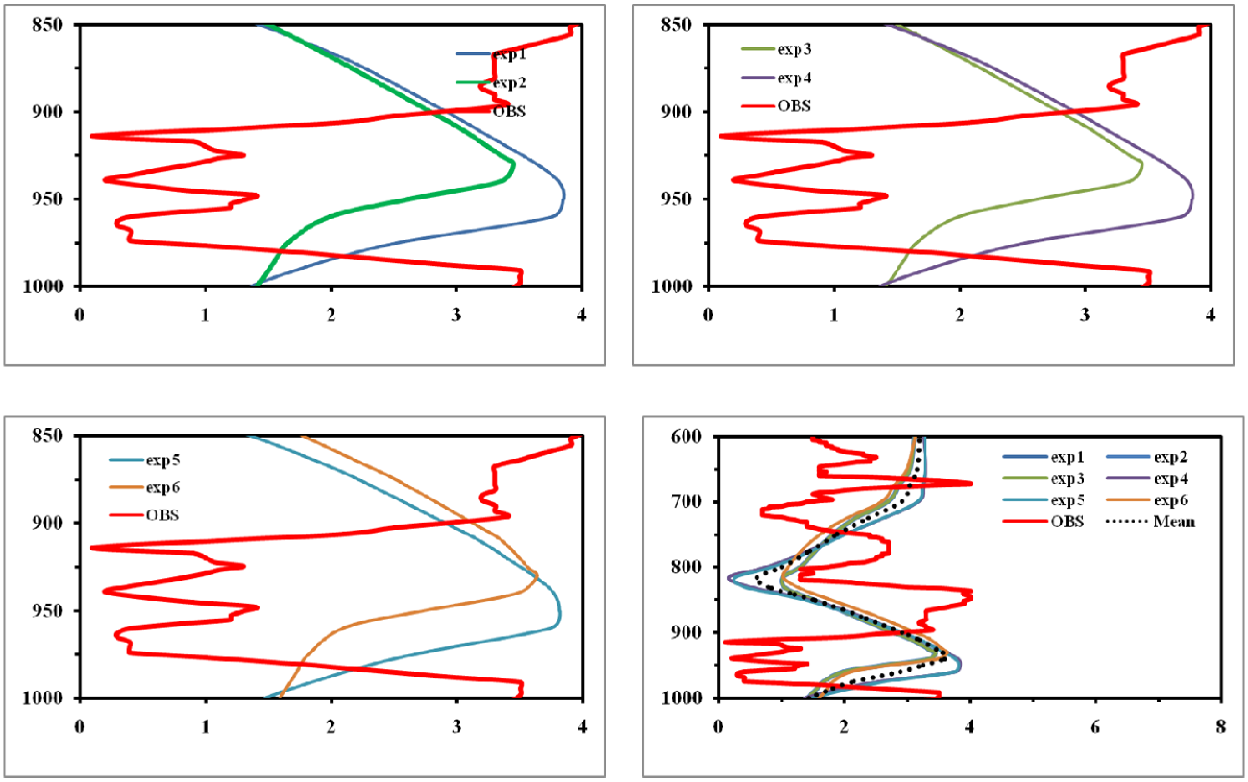

Figure 8. Model predicted vertical variation of relative humidity (%) for the different sensitivity experiments along with the observations at the location of Harrison County School corresponding to 20 UTC of 18 June 2009

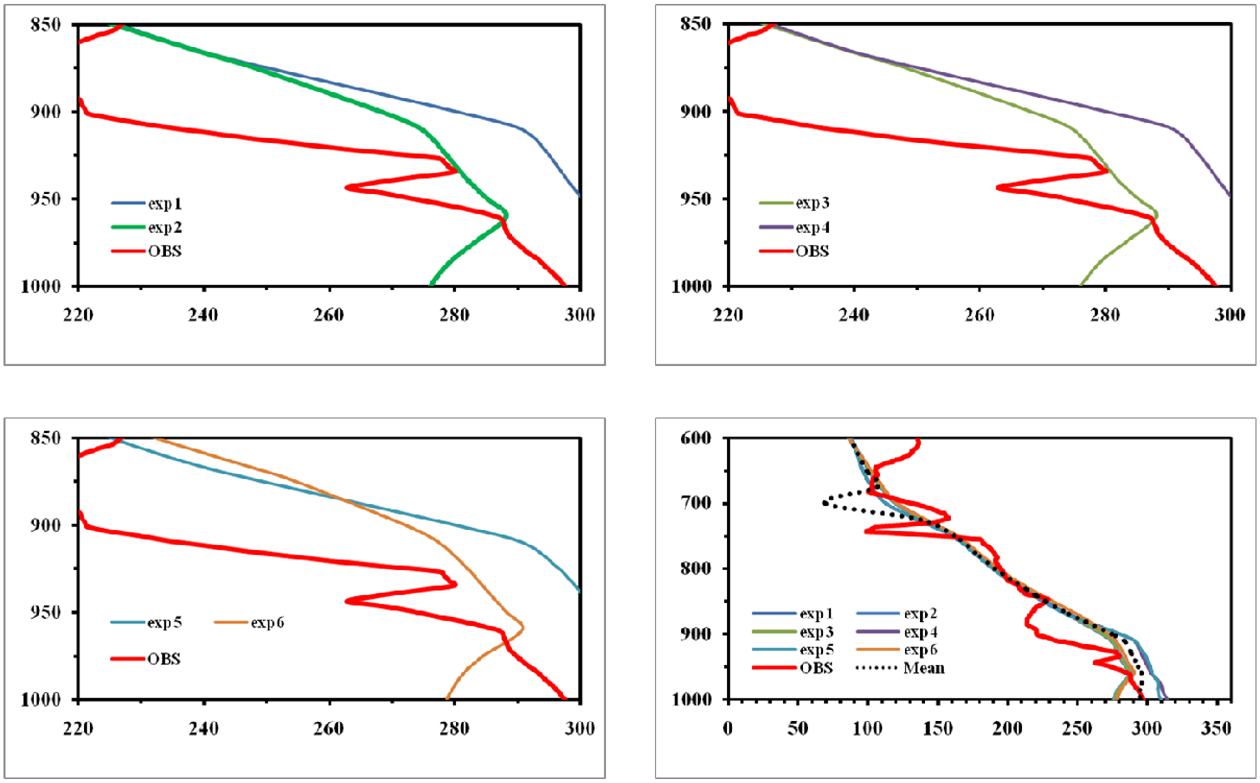

Figure 9. Model predicted vertical variation of wind direction for the different sensitivity experiments along with the observations at the location of Harrison County School corresponding to 14 UTC of 18 June 2009

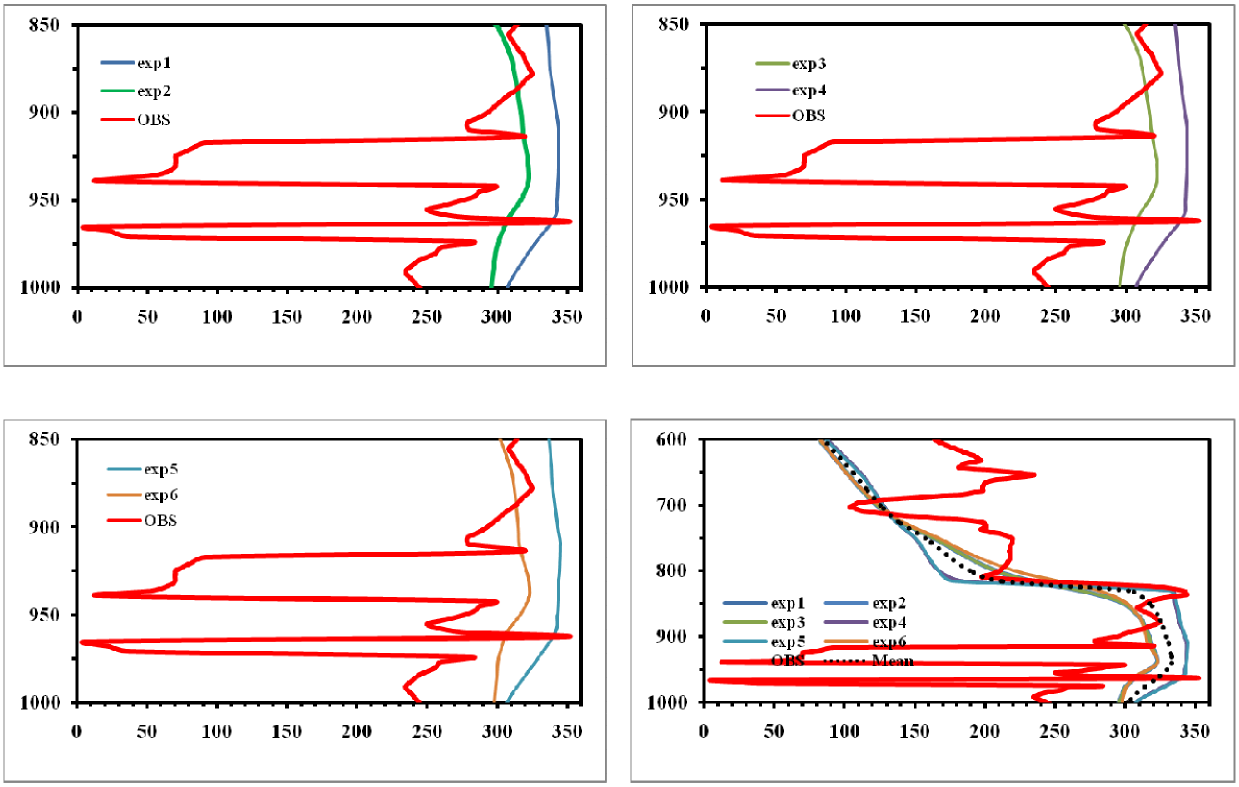

Figure 10. Model predicted vertical variation of wind direction for the different sensitivity experiments along with the observations at the location of Harrison County School corresponding to 20 UTC of 18 June 2009

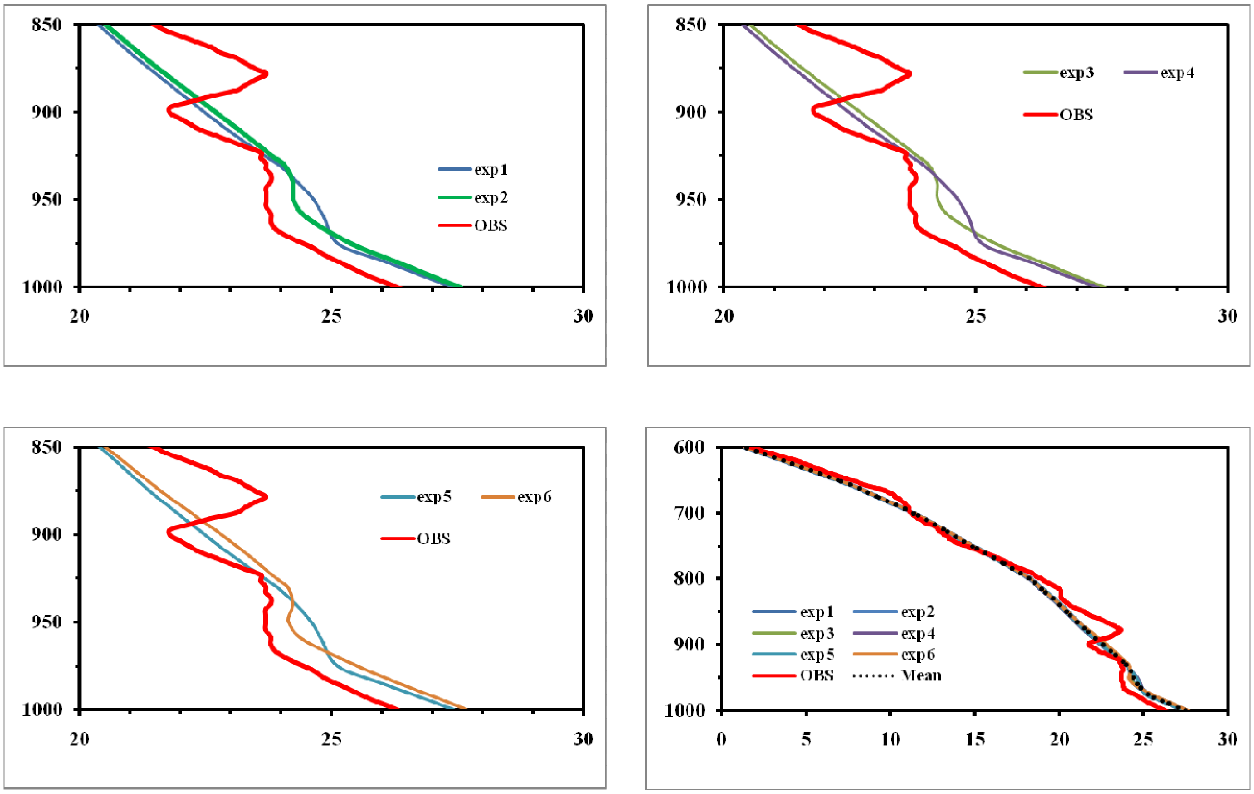

Figure 11. Model predicted vertical variation of temperature (C) for the different sensitivity experiments along with the observations at the location of Wiggins Airport corresponding to 14 UTC of 18 June 2009

2009061822 (T)

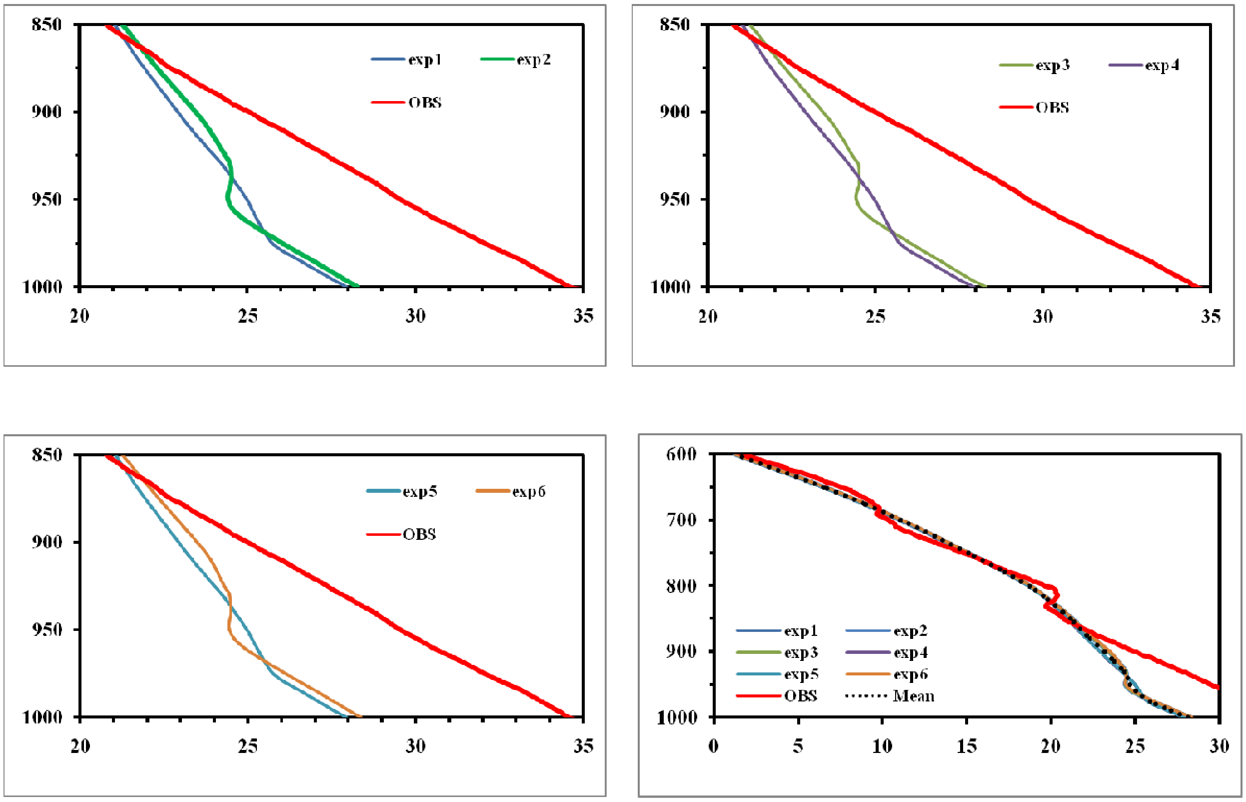

Figure 12. Model predicted vertical variation of temperature (C) for the different sensitivity experiments along with the observations at the location of Wiggins Airport corresponding to 20 UTC of 18 June 2009

2009061814 (RH)

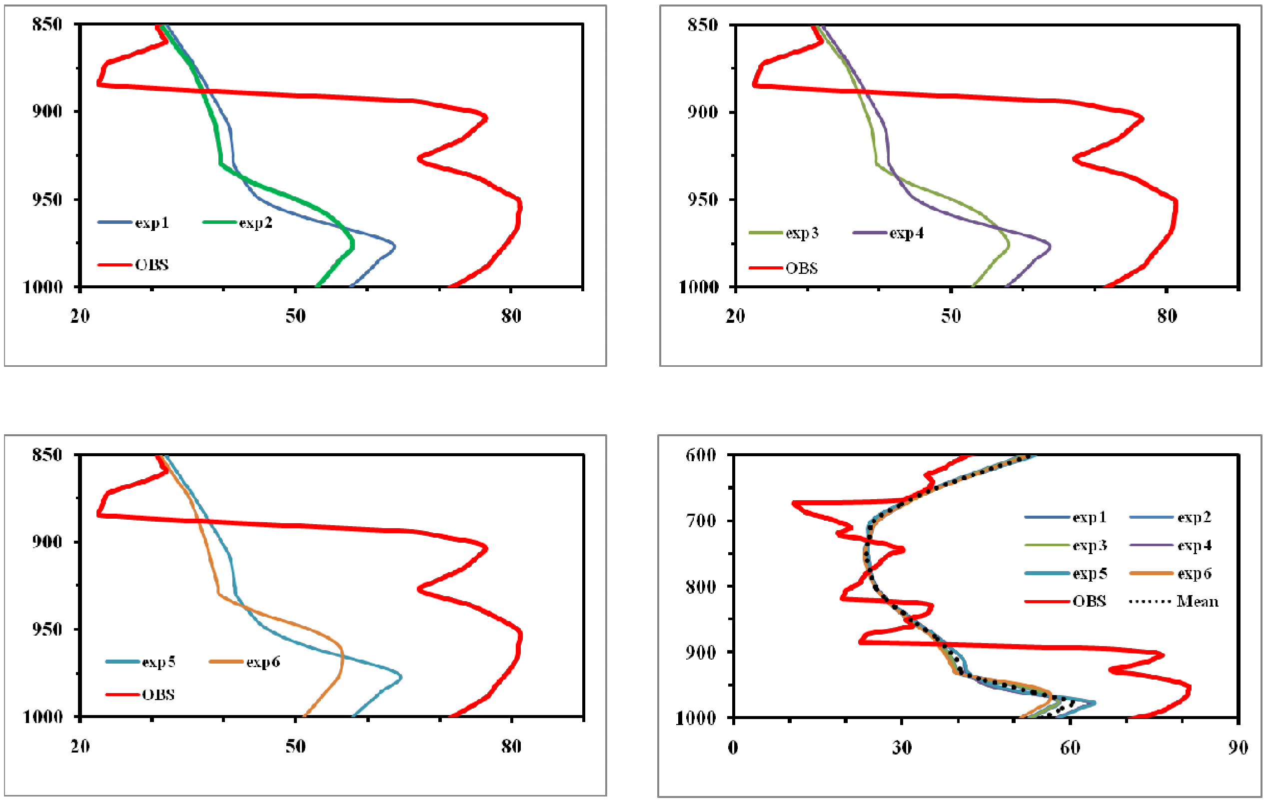

Figure 13. Model predicted vertical variation of relative humidity (%) for the different sensitivity experiments along with the observations at the location of Wiggins Airport corresponding to 14 UTC of 18 June 2009

2009061822 (RH)

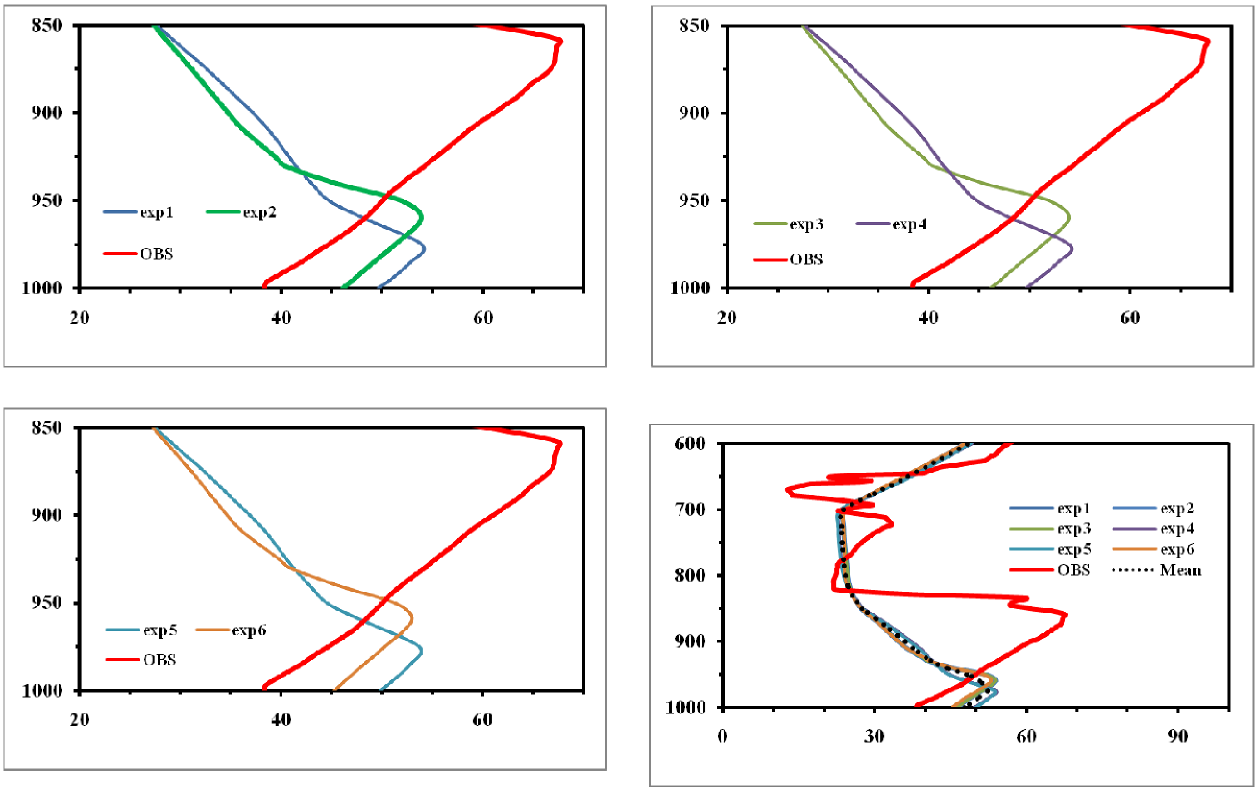

Figure 14. Model predicted vertical variation of relative humidity (%) for the different sensitivity experiments along with the observations at the location of Wiggins Airport corresponding to 20 UTC of 18 June 2009

Wind speed

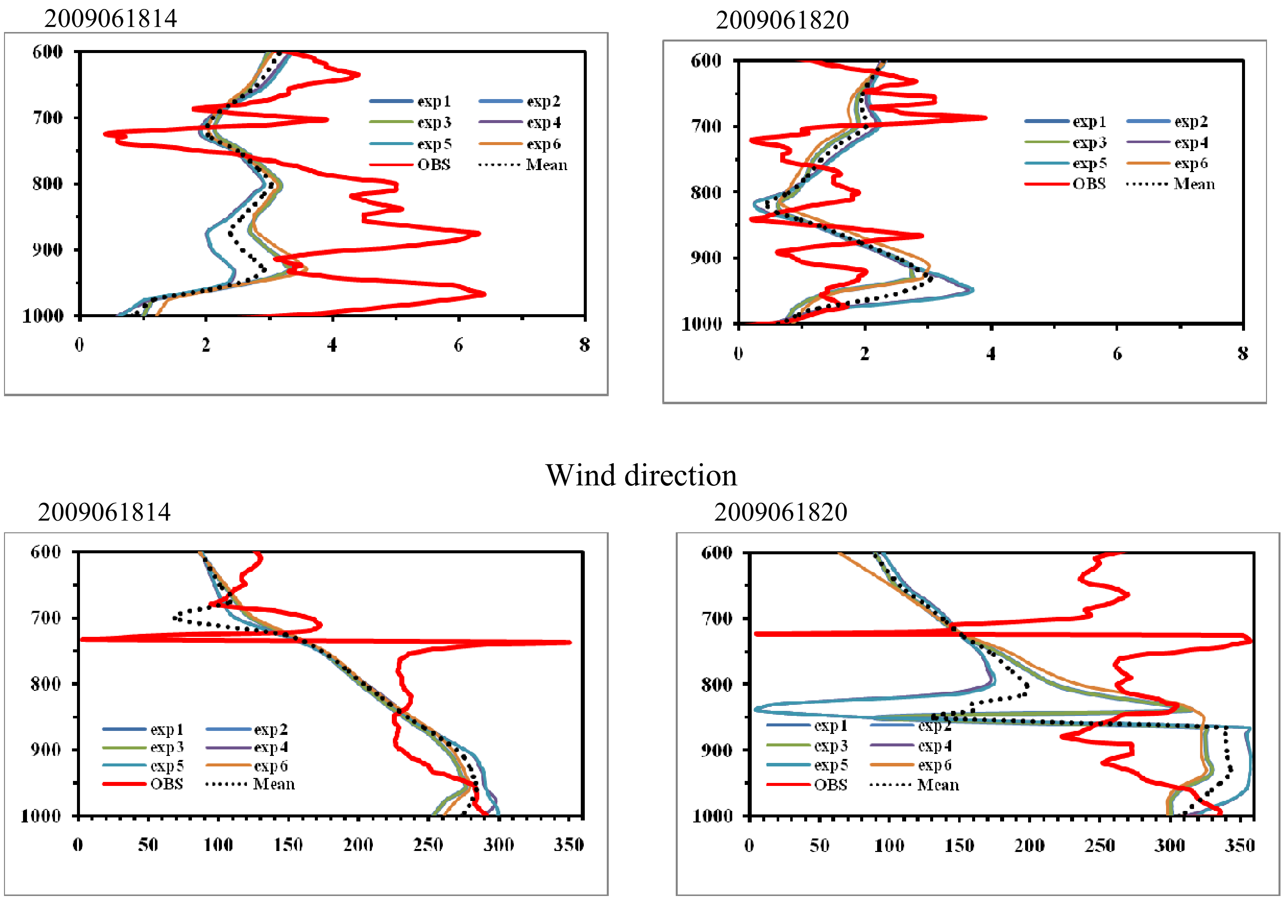

Figure 15. Model predicted vertical variation of wind speed (m/s) and wind direction for the different sensitivity experiments along with the observations at the location of Wiggins Airport. Top panel corresponds to wind speed and bottom panel corresponds to wind direction. Left panel corresponds to 14 UTC and right panel corresponds to 20 UTC of 18 June 2009.